TRANSACTIONS ON ELECTRICAL AND ELECTRONIC MATERIALS
Vol. 18, No. 1, pp. 46-50, February 25, 2017

Regular Paper

pISSN: 1229-7607 eISSN: 2092-7592
DOI: https://doi.org/10.4313/TEEM.2017.18.1.46
OAK Central: http://central.oak.go.kr

Paramagnetic $Zn_{(1-x)}Mn_xO$ (0.00≤x≤0.06) Nanoparticles Prepared by The Coprecipitation Method

Heru Harsono†
Department of Mechanical Engineering, Faculty of Engineering and Department of Physics, Faculty of Mathematics and Natural Sciences, Universitas Brawijaya, Malang 65145, Indonesia

I Nyoman Gede Wardana and Achmad As'ad Sonief
Department of Mechanical Engineering, Faculty of Engineering, Universitas Brawijaya, Malang 65145, Indonesia

Darminto
Department of Physics, Faculty of Mathematics and Natural Sciences, Institut Teknologi Sepuluh Nopember, Surabaya 60111, Indonesia

Received November 20, 2015; Revised October 25, 2016; Accepted November 1, 2016

The Zn1-xMnxO (0.00≤x≤0.06) samples have been synthesized in the form of powder by the coprecipitation method at low temperature using $Zn(CH_3COO)_2$. $2H_2O$ and $Mn(CH_3COO)_2$. $4H_2O$ powders, as well as HCl and NH_4OH solutions as starting materials. Characterization was conducted using XRD, TEM, XRF, FTIR and VSM. The result shows that the $Zn_{(1-x)}Mn_xO$ (0.00≤x≤0.06) nanoparticles have the wurtzite phase with a hexagonal structure and particle sizes ranging from 17.48 to 118.83 nm. In a qualitative analysis of XRF, the peaks that confirm the existence of the manganese element in Mn-doped ZnO samples were observed. Meanwhile, FTIR test result shows that there are peaks at around 500 cm^{-1} and 400 cm^{-1} in the FTIR spectra for Mn doped ZnO samples which clearly reveal the existence of the (Zn, Mn)-O strain mode. The (Zn, Mn)-O absorption peak positions have shifted to a lower wave number with increasing Mn doping content. The peak intensity is also lower if compared to that of the ZnO sample without doping. From the VSM test, it is shown that $Zn_{(1-x)}Mn_xO$ (0.00≤x≤0.06) nanoparticles are all paramagnetic having monotonically increased susceptibility as increasing Mn content.

Keywords: $Zn_{(1-x)}Mn_xO$ (0.00≤x≤0.06), Paramagnetic, Coprecipitation, Nanoparticles, Structure

1. INTRODUCTION

Magnetic nanoparticles are interesting materials because of their unique properties and important potential applications. Researchers have studied magnetic nanoparticles because they have different physical and chemical properties than the bulk material. Differences in physical and chemical properties are related to the existence of quantum size effects in the material [1].

† Author to whom all correspondence should be addressed:
E-mail: heru_har@ub.ac.id

Magnetization and isotropy of nanoparticles are different from the bulk material properties, and they have different Curie (T_c) and Neel (T_N) temperatures. Other interesting properties of magnetic nanoparticles are GMR (giant magnetoresistance), large magnetocaloric effect, and other properties. An unusual property of magnetic nanoparticles is their superparamagnetic behavior. This behavior appears in materials with a single order magnetic domain. Because of its small size, the material domain is highly reactive to an external magnetic field, but if the effect of the external magnetic field is removed, the behavior reverts to a paramagnetic material [2].

Because of the above mentioned properties, magnetic nanoparticles have been used in spintronics [3,4], photodiodes [5], photocatalysts [6], ultraviolet (UV) luminescent devices, light emitting diodes (LEDs), gas sensors, solar cells, and a transparent

thin film transistor [7,8]. These magnetic nanoparticles can easily be conjugated with functional molecules such as cells, enzymes, antibodies, DNA and RNA [9].

Great attention has been given to ZnO-based magnetic nanoparticles which are classified as an n-type intrinsic semiconductor with a band gap of 3.34 eV and an exciton binding energy of 60 MeV [10,11]. In recent years, the synthesis of ZnO and its doping with transition metal ions (Fi, Ne, Mn, Co, V, etc.) have been conducted by many researchers in nanotechnology [10] using a variety of methods, such as : spin coating [12] sol-gel [8,13], spray [14], metal organic deposition [15], radio frequency magnetron sputtering [16], pulsed laser deposition [17-19], and coprecipitation [20-22]. Among these methods, coprecipitation yields good control of particle size so that it produces samples on the order of nanometers. Coprecipitation is a simple, economical, energy efficient method because the process uses low temperatures and is environmentally friendly [23].

In this article, we report the successful synthesis of $Zn_{(1-x)}Mn_xO$ ($0.00 \le x \le 0.06$) nanopowders employing the coprecipitation method. For all the doping levels we introduced, the resulted powders were single phase and no impurity phase was identified. Although a number of researchers reported that at room temperature the magnetic properties of Mn-doped ZnO samples vary, both in ferromagnetic/superparamagnetic [24,25] and paramagnetic [17,26,27] properties, we observed an enhanced paramagnetism in all samples with x in the range from 0 up to 0.06.

2. EXPERIMENTS

2.1 Materials

The chemicals used were zinc acetate dihydrate $Zn(CH_3COO)_2.2H_2O$ (Merck,≥99%), manganese (II) acetate tetrahydrate $Mn(CH_3COO)_2.4H_2O$ (Aldrich Chemistry,≥99%), 37% HCl (Merck), and NH_4OH 25% (Merck).

2.2 Synthesis procedure

$Zn_{(1-x)}Mn_xO$ ($0.00 \le x \le 0.06$) nanoparticles were prepared by the coprecipitation method. The $Zn(CH_3COO)_2.2H_2O$ was mixed with $Mn(CH_3COO)_2.4H_2O$ based on stoichiometry calculations and dissolved in HCl (0.5 M, PA 99.9%). After that, a solution of NH_4OH_3 M was dripped to obtain a pH of 9. The solution was then stirred using a magnetic stirrer at 85°C for 6 hours. The precipitate in the solution was filtered and washed with distilled water until it was clean. Samples were then dried in an oven at 100°C for 3 hours and calcinated at 350°C for 3 hours.

2.3 Characterization

The as-prepared $Zn_{(1-x)}Mn_xO$ ($0.00 \le x \le 0.06$) nanoparticles were characterized by XRD (X-ray diffractometry) using a Phillips X-pert Powder Diffractometer with radiation source CuKα (λ=1.54056 Å). Phase identification analysis was conducted with the X'Pert High Score Plus program. Analysis of the diffraction pattern was undertaken with the Rietveld refinement method using the Rietica program to explore the crystal structure of the $Zn_{(1-x)}Mn_xO$ ($0.00 \le x \le 0.06$) sample. Transmission electron microscopy (TEM, JEOL-JEM 1400) and the spectrum of the X-Ray Fluorescence (XRF, PANalytical MiniPA14) from the $Zn_{(1-x)}Mn_xO$ ($0.00 \le x \le 0.06$) samples were employed to study the morphological characteristics and elemental content. Meanwhile, FTIR analysis using a spectrophotometer (FTIR-8400 S Shimadzu) was performed to observe the absorption peaks associated with the vibration frequency of atomic bonds in the $Zn_{(1-x)}Mn_xO$ ($0.00 \le x \le 0.06$) nanoparticles. The magnetic property was measured by a vibrating sample magnetometer (VSM type Oxford VSM1.2H).

3. RESULTS AND DISCUSSION

3.1 Structural analysis

The measured XRD patterns of the samples are given in Fig. 1, showing the crystallized nanoparticles corresponding to the main peaks at 2θ of around 36°. This correlates to the (011) diffraction plane of the zinc oxide in the hexagonal wurtzite phase.

This analysis is strengthened by other peaks having Miller indexes of (010), (002), (012), (110), (013), (020), (112), (021), (004) and (002). All Rietveld analyses utilizing Rietica have produced outputs with suitable parameters (measured by the figure of merit, or FoM,) in the form of GoF, Rp, RWP, and Re, which are acceptable (see Table 1) [28]. Thus, the data from the crystallography obtained from these analyses can be used for further discussion.

The crystallographic data which includes lattice parameters, crystal volume and density, as well as particle sizes resulting from Rietveld refinement analyses are given in Table 2. The values of crystallographic parameters generated in this study are close to those produced by Sharma, et al. [29]. Small shifts in lattice parameter values and crystal volume indicate the successful incorporation of Mn^{2+} ions into ZnO. Compared to ZnO without doping, the doped samples have slightly greater parameter values of lattices a and c and a slightly larger crystal volume. Along with the increasing concentration of Mn doping, the crystallographic parameters tend to increase. This structural change is caused by the fact that the radius of the Mn^{2+} ion (0.80 Å) is larger than that of Zn^{2+} (0.74 Å) in the wurtzite structure [30]. The Mn doping also lowers the density of the crystal, from 5.69 kg/m^3 (x=0.00) to 5.64 kg/m^3 (x=0.06). Based on the results of the Rietveld analysis, the average

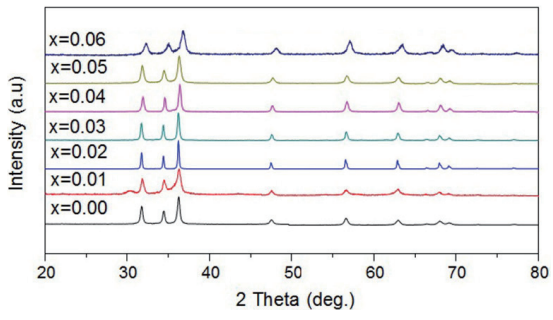

Fig. 1. The XRD patterns of all synthesized samples.

Table 1. Suitable parameters of rietveld-based rieticaanalysis.

Parameters		$Zn_{(1-x)}Mn_xO$						
		x=0.00	x=0.01	x=0.02	x=0.03	x=0.04	x=0.05	x=0.06
FoM	R_p(%)	8.82	13.84	9.68	8.71	8.95	6.91	12.23
	R_{wp}(%)	11.60	18.02	13.27	12.74	12.85	9.21	15.56
	R_e(%)	8.79	9.86	10.32	11.19	10.15	8.57	15.56
	GoF(%)	1.74	3.34	1.65	1,29	1.61	1.15	1.00

Table 2. Crystallographic data of $Zn_{(1-x)}Mn_xO$ (0.00≤x≤0.06) nanoparticles from rietveld refinement results.

Conc. (x)	a=b axis (Å)	c axis (Å)	Crystal volume (Å)^3	Density (kg/m^3)	Crystallite size (nm)
0.00	3.2479	5.1998	47.5039	5.69	34.85
0.01	3.2490	5.2078	47.6080	5.67	56.16
0.02	3.2500	5.2063	47.6231	5.66	118.83
0.03	3.2500	5.2053	47.6137	5.65	55.08
0.04	3.2498	5.2406	47.6037	5.69	41.04
0.05	3.2493	5.2056	47.5965	5.64	25.41
0.06	3.2506	5.1990	47.5751	5.64	17.48

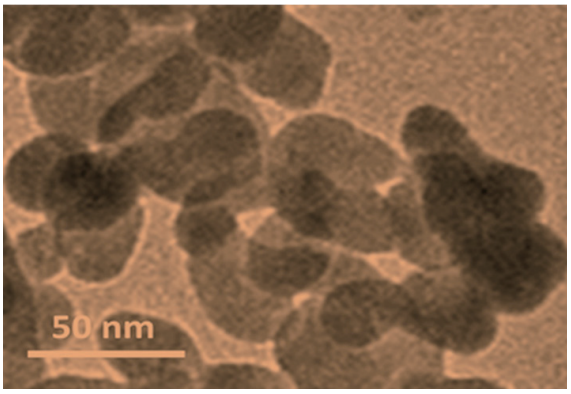

Fig. 2. TEM image of $Zn_{(1-x)}Mn_xO$ (x=0.01) nanoparticles.

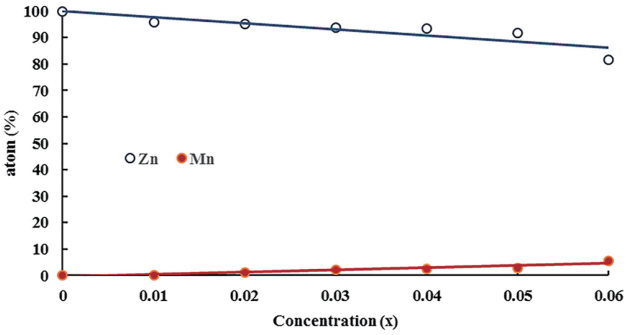

Fig. 3. The atomic contents of Zn and Mn resulting from the XRF examination compared to the starting composition of $Zn_{(1-x)}Mn_xO$.

size of crystal samples of $Zn_{(1-x)}Mn_xO$ (0.00≤x≤0.06) indicates that the synthesized samples are nano-sized materials.

The TEM image in Fig. 2 clearly shows rounded particles with a less homogeneous size distribution. The Mn doping has induced a change of particle shape, from the typical rod-like one of ZnO to a more rounded one, and also showing agglomeration. The particle distribution is non-uniform and the dimension is about 50 nm. Different particles cannot be distinguished very clearly due to the growth of granules. One may see the cavities that are formed among the granules matrix. The existence of cavities among the granules is due possibly to a group of $Zn_{(1-x)}Mn_xO$ particles where dopants are not uniformly distributed.

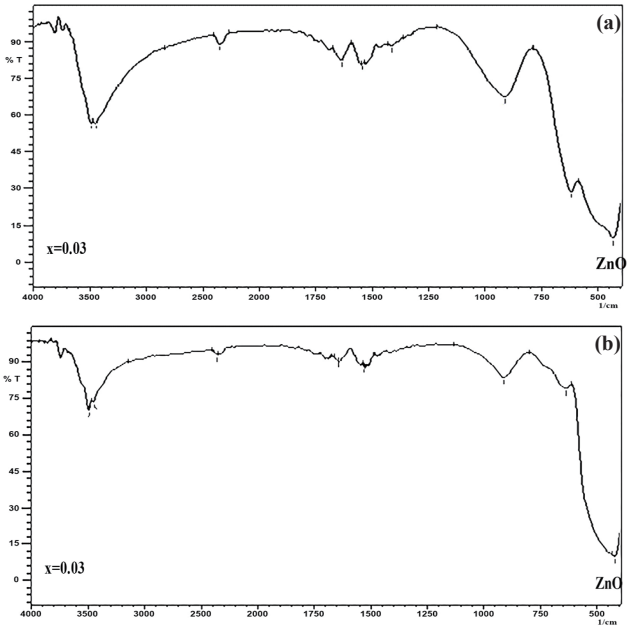

Fig. 4. FTIR spectra of $Zn_{(1-x)}Mn_xO$: (a) x=0.01 and (b) x=0.03.

The result of the qualitative analysis of the sample composition of nano particles $Zn_{(1-x)}Mn_xO$ (0.00≤x≤0.06) using XRF is shown in Fig. 3. It is observed that the percentage of zinc atoms (Zn) decreases with the increasing percentage of manganese atoms (Mn). The XRF characterization result also shows that the levels of manganese atoms (Mn) approach relatively the same levels during the synthesis of the samples of $Zn_{(1-x)}Mn_xO$ (0.00≤x≤0.06) nanoparticles, as compared to the starting materials.

3.2 Atomic bonding vibration mode analysis

Characterization by FTIR aims to identify the functional groups present in a compound. The data from FTIR spectra at wave numbers in the range of 400-900 cm^{-1} for $Zn_{(1-x)}Mn_xO$ (0.00≤x≤0.06) nanoparticles is shown in Fig. 4.

Table 3 represents the quantitative values of the absorption peak and functional groups for all doping concentration of Mn. Two main absorption peaks are at about 1,600 cm^{-1} and 1,400 cm^{-1} which refer to the carboxyl strain group (C=O) [31] and vibration Zn-C-O [21]. Absorption peaks around 3,500 cm^{-1} and 900 cm^{-1}, which correspond to strain vibration of O-H group of H_2O [32], suggest the presence of water absorbed on the surface of ZnO and deformation of C=O [33]. A peak at about 2,300 cm^{-1} is retained by CO_2 vibration due to its presence in the air [11]. Another peak at around 650 cm^{-1} due to a symmetric bending of O-H [32] is also observed.

Importantly, a very strong band is detected at 487.96 cm^{-1} in the FTIR spectrum for ZnO without doping which is most likely due to

Table 3. The functional groups of $Zn_{(1-x)}Mn_xO$ (0.00≤x≤0.06) nanoparticles produced by coprecipitation method.

Functional group	x=0.00	x=0.01	x=0.02	x=0.03	x=0.04	x=0.05	x=0.06
O-H stretching	3494.77	3496.70	3494.77	3492.85	3434.98	3454.27	3436.91
CO_2 vibration	2339.49	2360.71	2364.57	2360.71	2343.35	2341.42	2339.49
C=O stretching	1550.66	1550.66	1512.09	1525.59	1623.69	1542.95	1517.87
Zn-C-O vibration	1460.01	1406.01	1407.94	absent	absent	1396.37	1398.30
C=O deformation	916.12	921.91	906.48	910.34	906.48	933.48	923.84
O-H sym.bending	725.18	717.47	absent	636.47	514.96	absent	absent
Zn-O stretching	487.96	468.47	443.60	416.60	437.81	428.17	424.31

the Zn-O strain mode [32]. Other peaks at around 500 cm^{-1} and 400 cm^{-1} in FTIR spectra for Mn doped ZnO clearly reveal the presence of the (Zn,Mn)-O strain mode [18]. The (Zn,Mn)-O absorption peaks decrease along with the increase of Mn doping and the value is lower if compared with ZnO nanoparticles without doping. Overall, the absorption peaks indicate the presence of resonant interaction among the vibrational modes of oxide ions in $Zn_{(1-x)}Mn_xO$ nanoparticles.

3.3 Magnetic properties

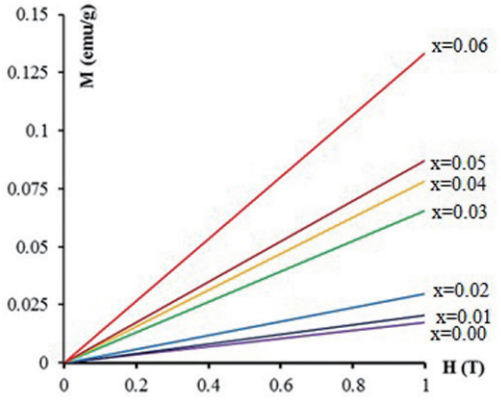

Fig. 5. The M - H curves of $Zn_{(1-x)}Mn_xO$ (0.00≤x≤0.06).

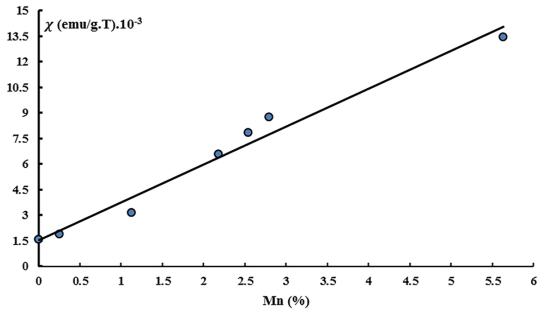

Fig. 6. Plot of the effect of the percentage of Manganese atoms on the value of magnetic susceptibility.

To determine the magnetic properties of $Zn_{(1-x)}Mn_xO$ (0.00≤x≤0.06) nanoparticles, characterization was conducted by using a VSM (vibrating sample magnetometer) at room temperature. The examination was carried out using an external magnetic field ranging from 0 to 1 tesla (T) at room temperature. The result is shown in Fig. 5.

The linear curve in Fig. 5 indicates that all samples of $Zn_{(1-x)}Mn_xO$ (0.00≤x≤0.06) are paramagnetic, being monotonically enhanced with increasing Mn-doping level. When the magnetic susceptibility is plotted against the Mn content, one may see a linear curve as shown in Fig. 6. We use the actual Mn content from the XRF analysis (Fig. 3) of the as-prepared samples to plot the curve.

Elanchezhiyan, et al. [26] also reported paramagnetism in $Zn_{(1-x)}Mn_xO$ thin films with a higher doping level of Mn (x=0.05, 0.10 and 0.15). Due to the fact that no second phase is detectable in their samples as well as in ours, the magnetic moment may only come from the Mn ions as dopants. The paramagnetic property shows a lack of interaction between magnetic moments of Mn ions at room temperature, as long as there are no other defects or impurities creating additional magnetic moments. In contrast, the Mn-doped ZnO has so far exhibited ferromagnetism, superparamagnetism and even diamagnetism, as reported previously [24,25,29]. These pose questions for further study.

4. CONCLUSIONS

$Zn_{(1-x)}Mn_xO$ (0.00≤x≤0.06) nanoparticles having a single hexagonal wurtzite phase have been successfully synthesized by the coprecipitation method at low temperature. The smallest crystal size of around 17.48 nm and the largest one of about 118.83 nm have been achieved for the samples with x=0.06 and 0.02 respectively. The magnetic measurement reveals that the $Zn_{(1-x)}Mn_xO$ (0.00≤x≤0.06) nanoparticles exhibit paramagnetism. The magnetic susceptibility linearly increases with increasing Mn content of the nanoparticles.

ACKNOWLEDGMENTS

This work was partly supported by UB (universitas brawijaya) and the Institut Teknologi Sepuluh Nopember (ITS). One of the authors (Heru Harsono) is grateful for supports from UB (universitas brawijaya) and the Ministry of Technology Research and Higher Education of the Indonesian Republic in providing a BPPDN scholarship for his doctoral program.

REFERENCES

[1] S. P. Gubin, Y. A. Koksharov, G. B. Khomutov, and G. Y. Yurkov, *Russian Chemical Reviews*, **74**, 489 (2005).
[2] A. Wu, P. Ou, and L. Zeng, *Nano*, **5**, 245 (2010). [DOI: https://doi.org/10.1142/S1793292010002165]
[3] C. Ronning, P. X. Gao, Y. Ding, and L. Wang., *Appl. Phys. Lett.*, **84**, 783 (2004).
[4] X. Luo, W. T. Lee, G. Xing, N. Bao, A. Yonis, D. Chu, J. Lee, J. Ding, S. Li, and J. Yi, *Nanoscale Res. Lett.*, **9**, 1 (2014).
[5] L. Luo, Y. Zhang, S. S. Mao, and L. Lin, *Sens. Actuators A.*, **127**, 201 (2006).
[6] S. D. Puckett, E. Taylor, T. Raimondo, and T. J. Webster, *Biomaterials*, **31**, 706 (2010). [DOI: https://doi.org/10.1016/j.biomaterials. 2009.09.081].
[7] J. E. Ghoula, C. Barthoub, and L. E. Mir, *Physica E : Lowdimensional Systems and Nanostructures*, **44**, 1910 (2012). [DOI: https://doi.org/10.1016/j.physe.2012.05.020]
[8] A. K. Zak, W.H.A. Madjid, M. E. Abrishami, R. Yousefi, and R. Parvizi, *Solid State Science*, **14**, 488 (2012). [DOI: https://doi.org/10.1016/j.solidstatesciences. 2012.01.019]
[9] P. S. D'Agostino, Ph. D., Universita degli Studi di Modena e Reggio Emilia, Italy (2009).
[10] Y. M. Hao, S. Y. Luo, S. M. Zhou, R. J. Hao, G. Y. Zhu, and N. Li, *Nanoscale Res. Lett.*, **7**, 1 (2012). [DOI: https://doi.org/10.1186/1556-276X-7-100]
[11] M. E. Abrishami, S. M. Hosseini, E. A. Kakhki, A. Kompany, and M. Ghasemifard, *International Journal of Nanoscience*, **9**, 19 (2010). [DOI: https://doi.org/10.1142/S0219581X1000648X]
[12] D. A. Schwartz, N. S. Norberg, Q. P. Nguyen, J. M. Parker, and D. R. Gamelin, *Journal of the American Chemical Society*, **9**, 13205 (2003). [DOI: https://doi.org/10.102/ja036811v]
[13] L. Zhifeng, L. Chengcheng, Y. Jiang, and E. Lei, *Solid State Sciences*, **12**, 111 (2010). [DOI: https://doi.org/10.1016/j.solidstatesciences. 2009.10.014]
[14] V. R. Shinde, T. P.Gujar, C. D. Lokhande, R. S. Mane, and S. H. Han, *Mater. Chem. Phys.*, **96**, 326 (2006). [DOI: https://doi.org/10.1016/j.matchemphys.2005.07.045]
[15] A. C. Tuan, J. D. Bryan, A. B. Pakhomov, V. Shutthanandan, S. Thevuthasan, D. E. McCready, D. Gaspar, M. H. Engelhard, J. W. Rogers Jr., K. Krishnan, D. R. Gamelin, and S. A. Chambers, *Phys. Rev. B*, **70**, 054424 (2004). [DOI: https://doi.org/10.1103/PhysRevB.70.054424]

[16] A. Atsushi, N. Takahiro, and F. Norifumi, *J. Appl. Phys.*, **99**, 013509 (2006). [DOI: https://doi.org/10.1063/1.2150596]
[17] A. Tiwaria, C. Jina, A. Kvita, D. Kumar, J. F. Muth, and J. Narayana, *Solid State Communications*, **121**, 371 (2002). [DOI: https://doi.org/10.1016/S0038-1098(01)00464-1]
[18] K. Ando, H. Saito, Z. Jin, T. Fukumura, M. Kawasaki, Y. Matsumoto, and H. Koinuma, *J. Appl. Phys.*, **89**, 7284 (2001). [DOI: https://doi.org/10.1063/1.1356035]
[19] T. Fukumura, Z. W. Zin, A. Ohtomo, H. Koinuma, and M. Kawasaki, *Appl. Phys. Lett.*, **75**, 3366 (1999). [DOI: https://doi.org/10.1063/1.125353]
[20] M. A. Shafique, S. A. Shah, M. Nafees, K. Rasheed, and R. Ahmad, *International Nano Lett.*, **2**, 1 (2012). [DOI: https://doi.org/www. inl-journal.com/content/2/1/31]
[21] S. Bagheri, K. G. Chandrappa, and S.B.A. Hamid, *Der Pharma Chemica*, **5**, 265 (2013). [DOI: https://doi.org/ derpharmachemica.com/ archive.html]
[22] T. L. Tan, C. W. Lasi, W. L. Chin, and S.B.A. Hamed, *J. Nanomater.*, **2014**, 1 (2014). [DOI: https://doi.org/ 10.1155/2014/371720]
[23] F. Chekin, S. Bagheri, and S. B. A. Hamid, *Analytical Methods*, **4**, 2423 (2012). [DOI: https://doi.org/10.1039/C2AY25251A]
[24] S. W. Jung, S. J. An, G. C. Yi, C. U. Jung, S. I. Lee, and S. Cho, *Appl. Phys. Lett.*, **80**, 4561 (2002).
[25] L. B. Duan, G. H. Rao, J. Yu, Y. C. Wang, W. G. Chu, and L. N. Zhang, *J. Appl. Phys.*, **102**, 103907 (2007).
[26] J. Elanchezhiyan, P. Bhuvana, N. V. Gopalakrishnan, A. Thamizhavel, and T. Balasubramanian, *Z. Naturforsch*, **63a**, 585 (2008).
[27] X. M.Cheng and C. L. Chien, *J. Appl. Phys.*, **93**, 7876 (2003).
[28] B. A. Hunter, *Rietica - A visual Rietveld program*, **20**, 21 (1998).
[29] R. K. Sharma, P. Sandeep, and K, C. Pargaien, *Adv. Nat. Sci.: Nanosci. Nanotechnol.*, **3**, 1 (2012).
[30] J. Anghel, A. Thurber, D. A. Tenne, C. B. Hanna, and A. Punnoose, *J. Appl. Phys.*, **107**, 09E314 (2010).
[31] M. E. Abrishami, S. M. Hosseini, E. A. Kakhki, A. Kompany, and M. Ghasemifard, *International Journal of Nanoscience*, **9**, 19 (2010). [DOI: https://doi.org/10.1142/S0219581X1000648X]
[32] B. N. Dole, V. D. Mote, V. R. Huse, Y. Purushotham, M. K. Lande, K. M. Jadhav, and S. S. Shah, *Current Appl. Phys.*, **11**, 762 (2011). [DOI: https://doi.org/www.elsevier.com/locate/cap]
[33] N. F. Djaja and R. Saleh, *Mater. Sci. Appl.*, **3**, 245 (2012). [DOI: https://doi.org/10.4236/msa.2012.34036]